DESIGN FOR THE DIAMOND LONGITUDINAL BUNCH-BY-BUNCH FEEDBACK CAVITY

A. F. D. Morgan, G. Rehm
Diamond Light Source, Oxfordshire, UK

ABSTRACT

In 2017 it is planned to install some additional normal conducting cavities into the Diamond storage ring. In order to deal with the potential higher order modes in these, we are designing a longitudinal bunch-by-bunch feedback system. This paper will focus on the design of the overloaded cavity kicker, adapted to the Diamond beam pipe cross section. The design has evolved in order to reduce the strong 3^{rd} harmonic resonance seen on the introduction of the racetrack beam pipe. Through a combination of geometry optimisation and the addition of integrated taper transitions this harmonic has been greatly reduced while also minimising sharp resonances below 15 GHz. The major features will be described, as well as the expected performance parameters.

DESIGN

The design comprises a pillbox cavity, with additional coaxial ports coupled via ridged waveguides. In a development on our previous work, the design frequency was moved to 1.875 GHz from the lower 1.625 GHz. This was in order to move more of the higher order modes (HOMs) above the cutoff frequency of the beam pipe and to space out the remaining lines. 2.125 GHz was also considered, but found to generate additional lower frequency HOMs in the structure.

Theoretically, the ridged waveguide structure and the waveguide to coaxial transition both act as high pass filters, and care must be taken to make sure that the overall cutoff frequency is low enough such that all of the higher order modes can be coupled out of the cavity. In practice they behaved more like band pass filters, so the aim was to extend the pass band to as high a frequency as possible.

The coupling structures were originally modelled separately, in order to iterate the model faster. Figure 1 shows a representation of the modelled geometry. The best result was then incorporated into the full model. Figure 2 shows the transmission through the waveguide and coaxial structures. The pass band extended from 1.8 GHz to 8 GHz. Although not ideal it was decided that it was good enough to be incorporated into the full model.

Although useful starting points can be obtained by modelling elements separately, the optimisation must be done on the full model so as to take into account of the interactions between elements. As an example, even with the waveguide and coaxial coupler optimised, there were still unwanted resonances in the wake impedance of the full model. With the original cavity, pipe and couplers, tuning the geometry in various ways could not achieve overall suppression of the

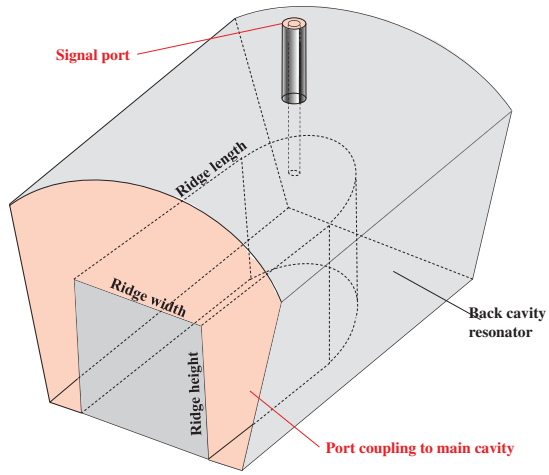

Figure 1: Sketch of the coupler geometry.

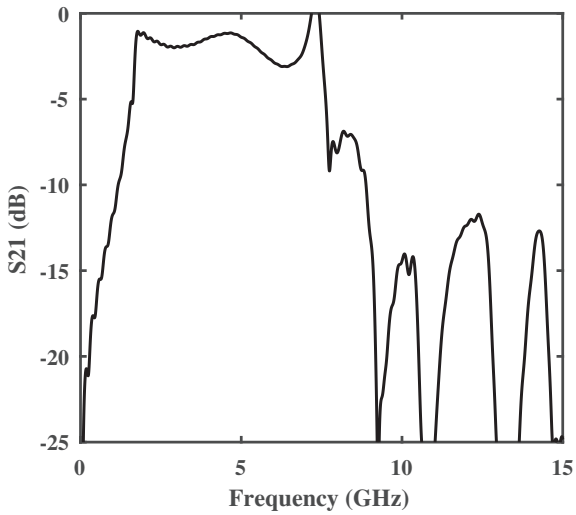

Figure 2: The transmission through the coupling structures as initially added to the full model.

HOM resonances. If one set of resonances was suppressed then another was enhanced.

Only when tapers were added to the model was the overall suppression of these unwanted features realised. After some investigation it was found that tapers moving from the Diamond standard racetrack profile on outer ends of the structure, to a circular profile at the central cavity performed best. Tapers were resisted originally as they are known to

ISBN 978-3-95450-177-9

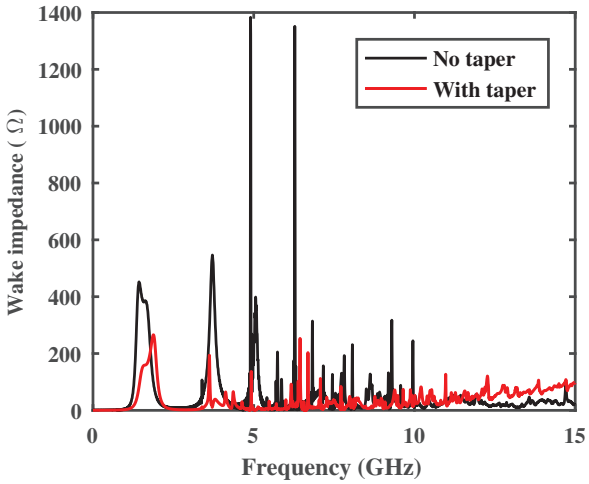

Figure 3: Adding the tapers gave sufficient overall HOM suppression.

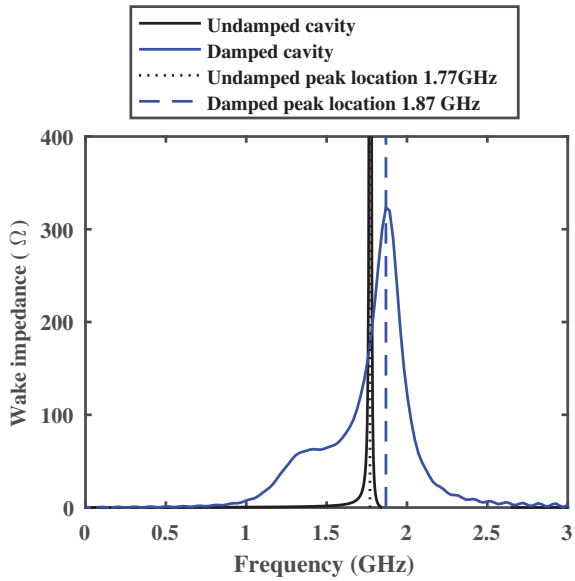

Figure 4: The addition of damping structure moves the resonance frequency from 1.77 GHz to the target of 1.87 GHz.

add additional harmonics lines [1], however with careful tuning of the taper angle the damping effects on the original unwanted harmonics was stronger than the unwanted harmonics introduced by the taper. Fortunately as the tapers were integrated directly into the design, longer, lower angle tapers were able to be used. Figure 3 shows an example of the HOM suppression achieved by adding the tapers.

One detrimental effect of adding the tapers was that the floor of the wake impedance began to rise above a particular frequency. In the case of Fig. 3 this can be seen starting at around 9 GHz. By keeping the tapers shallow the start of this rise was pushed up to around 15 GHz which was deemed acceptable as there is very little beam power at and above those frequencies.

The main cavity radius is defined by the target resonance desired. The cavity radius of the full design is different from that of a simple pillbox cavity due to the waveguides and transitions connecting the main cavity to the ports (see Fig. 4). This again highlighted the need to model the full structure early in the design process.

The curved ends of the coupling waveguide ridge remained curved, similar to the LNLS design [2], for the same reasons of improving the coupling between the ridged waveguide and the coaxial line. However it was found that changing the base of the ridged waveguide and back cavity resonator to be flat rather than following the radial curve had the effect of broadening the bandwidth, and suppressing some of the spikes introduced by adding the taper.

The exact amplitudes of the HOM resonances are somewhat dependent on the level of meshing used and the details of the feedthrough structure and ceramic behaviour. However, investigations showed that in terms of the meshing, finer meshing tended to reduce the amplitudes.

The feedthroughs are specified to be 50 Ω parts. The ceramic is AlO_3, but for the loss calculation, the tangent δ was unknown for this particular ceramic. In this case, the tangent δ of the most similar ceramic was used.

Once the design changes were implemented, another round of optimisation was done so that performance could be maximised. Once a final design was decided upon, a series of sensitivity scans were performed on the geometric parameters in order to identify those most sensitive to changes. As expected, the gap above the ridge in the coupling waveguide proved the most sensitive, changing the peak wake impedance in the operation band by 25 Ω per 100 μm. Increasing the peak impedance in this way had the cost of reducing the bandwidth, so the mechanical tolerance was reduced in order to achieve the balance between the two operating requirements found in the design process. The nose stub (see Fig. 6) also needed additional consideration as it moved the peak frequency. Less sensitive but still needing care was the ridge depth and length as deviations of 800 μm had the potential to enhance particular HOMs (see Fig. 1).

In order to close the loop in the design process, the mechanical drawings were exported as STL files and imported into both GdfidL [3] and CST [4] modelling software. This was then compared with the results from the final design written in native GdfidL input code. The agreement was very good giving us confidence that the mechanical drawings accurately represent our requirements (see Fig. 5).

PERFORMANCE

An overview of the final design is shown in Fig. 6. It will be constructed of three sections. The upstream and down stream sections contain the coupling structures and the tapers, and are shown in fig. 7. These slot into a middle

ISBN 978-3-95450-177-9

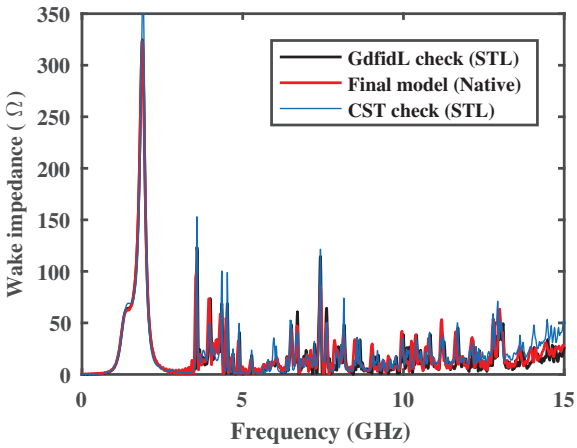

Figure 5: The comparison of the final EM model and the resulting mechanical drawings.

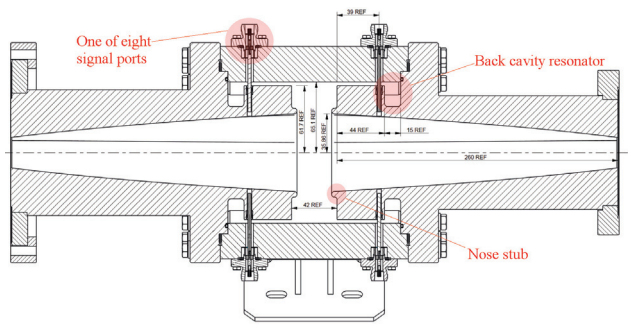

Figure 6: Slice view of the final cavity design.

section to form the main cavity. RF fingers are used to maintain good isolation between adjacent couplers.

The minimum wake impedance within the operational band is 137 Ω, as shown in fig. 8, which implies a minimum shunt impedance of 274 Ω [5]. The peak wake impedance is 306 Ω giving a peak shunt impedance of 612 Ω.

From our analysis of the energy loss in the structure [6], we know that most of the energy lost from the beam is emitted

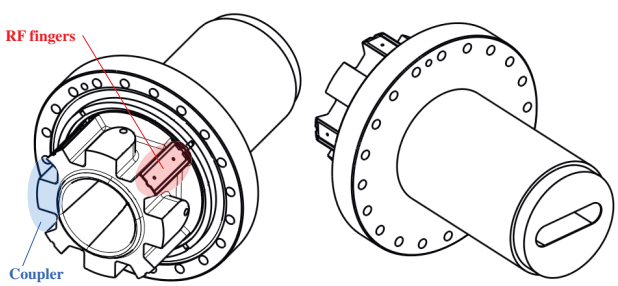

Figure 7: 3D representations of the upstream and downstream section. With a 90 degree angle for ease of viewing.

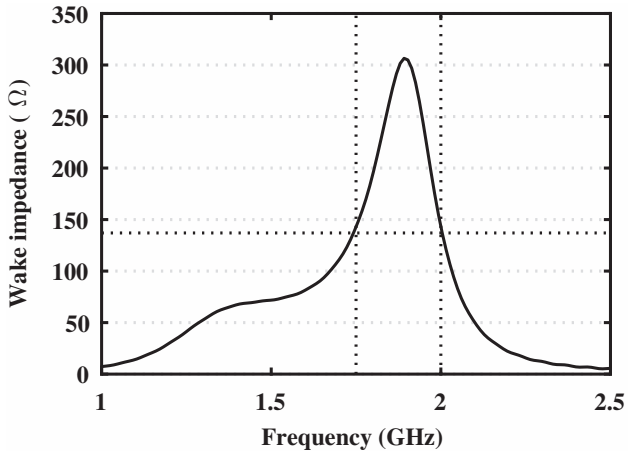

Figure 8: The wake impedance around the operating frequency. The dashed vertical lines show the operating region while the dashed horizontal lines show the minimum wake impedance.

Table 1: The Vast Majority of the Power is Extracted by the Signal Ports

Component	Power loss (%)
Beam ports	15
Signal ports	77
Cavity surface	7.7
Coaxial pin	0.3
Feedthrough ceramic	~0

out of the signal ports. Of the 8% lost into the cavity, the vast majority is lost across the internal surface. Very little is lost in the coaxial pins and feedthrough ceramic (see Table. 1). This has implications for the analog chain as there is potentially substantial power sent to the amplifier from the cavity. The plan is to use circulators to redirect this beam induced power safely into a high power load.

Because the bunch spectrum changes with operational conditions, and machining tolerancing can move the resonance frequencies by small amounts, we used a basic $P = I^2R$ relationship to estimate a worst case scenario of power coupled from the beam. The wake impedance was separated into sections each containing a single RF harmonic (500 MHz, 1 GHz, 1.5 GHz etc.). The maximum wake impedance for each section was found and combined with the expected current in that frequency range, based on a gaussian roll off which mimics the frequency behaviour of the beam. Table 2 summarises the results of this approach.

Table 2: Worst Case Beam Induced Power Estimates

	Frequency ranges (GHz)		
Operating current	0-1.75	1.75 - 2.25	2.25 - 15.25
300 mA	17 W	25 W	35 W
500 mA	47 W	71 W	98 W

ISBN 978-3-95450-177-9

Table 3: More Realistic Case Beam Induced Power Estimates

Operating current	Frequency ranges (GHz) 0-1.75	1.75 - 2.25	2.25 - 15.25
300 mA	8 W	12 W	10 W
500 mA	22 W	32 W	28 W

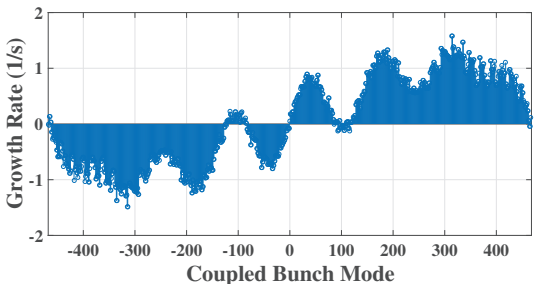

Figure 9: The growth rate of the coupled bunch modes.

For a 500 mA beam this basic approach gave 71 W coupled out in the operational band, and 98 W at frequencies above that, up to 15 GHz. For our usual operating current of 300 mA, these numbers reduce to 25 W in the operational band and 35 W for the HOMs. As this represents all modes in each section coupling as much as the worst mode in that section, this is an unrealistically pessimistic scenario. However, this upper bound means that we are comfortable that the analog chain, which is specified to cope with 200 W of power, will be suitably robust. In reality we expect the power load to be lower away from the operating band, as one is unlikely to hit all the strong resonances simultaneously. By running the same type of analysis but this time using the mean value of wake impedance for each section, the contribution from the general background is more clearly seen (see Table 3).

The impact of installing the cavity was investigated using a modified version of calculations in MatLab [7] obtained from LNLS, based on the Wang formalism [8]. This predicts the expected growth rate of coupled bunch modes caused by the cavity. For this design the maximum instability growth rate was 1.5/s implying a growth time of 370000 turns for current operating conditions. The effects of increasing the stored current from 300 mA to 500 mA was also investigated, but the maximum growth rate only increases to a still small value of 4/s. Figure 9 show the typical result under normal conditions.

The transverse wakes were also checked, as shown in figure 10, and found to be a benign 20 Ω/mm, which is of the same order as many other existing components.

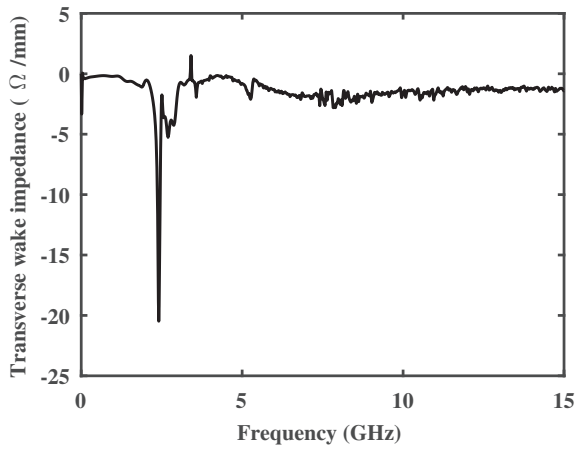

Figure 10: The transverse wake of the cavity.

CONCLUSION

A longitudinal feedback cavity has been designed for use in the Diamond storage ring. The design is highly damped in order to achieve the required bandwidth. It also has integral tapers in order to counteract the detrimental effect of the size and shape of the Diamond beam pipe through the cavity. Checks have been done on the expected impact on the ring after installation and they are expected to be minimal.

The authors would like to thank Richard Fielder for doing the comparison modelling in CST.

REFERENCES

[1] A. F. D. Morgan, G. Rehm, *Initial work on the design of a longitudinal bunch-by-bunch feedback kicker at diamond*, IBIC 2015.

[2] L. Sanfelici et.al., *Design and impedance optimisation of the LNLS-UVX longitudinal kicker cavity*, IBIC 2013.

[3] http://www.gdfidl.de

[4] http://www.cst.com

[5] D. A. Goldberg and G. R. Lambertson., *Dynamic devices: A primer on pickups and kickers*, AIP Conf. Proc. 1992 Vol.249 p 537.

[6] A. F. D. Morgan, G. Rehm, *Considerations and improved workflow for simulation of dissipated power from wake losses*, IBIC 2015.

[7] http://www.mathworks.com

[8] M. Wang, *Longitudinal symmetric coupled bunch modes*, BNL-51302.

ISBN 978-3-95450-177-9